

DESIGN AND TESTING ELEVATED STEEL FIBRE REINFORCED SELF-COMPACTING CONCRETE SLABS

Barros, J.A.O.^{*}, Salehian, H.^{**}, Pires, N.M.M.A.[†], Gonçalves, D.M.F.^{††}

^{*} ISISE, Dep. Civil Eng., School Eng., University of Minho
Campus de Azurém 4800-058 Guimarães, Portugal
e-mail: barros@civil.uminho.pt, web page: www.isise.net

^{**} ISISE, Dep. Civil Eng., School Eng., University of Minho
Campus de Azurém 4800-058 Guimarães, Portugal
e-mail: salehian@civil.uminho.pt, web page: www.isise.net

[†] Casais Company, Mire de Tibães, Braga, Portugal
e-mail: miguel.pires@casais.pt, web page: www.casais.pt/

^{††} CiviTest Company, Vila Nova de Famalicão, Portugal
e-mail: delfinagoncalves@civitest.com, web page: www.civitest.pt

Keywords: fibre reinforced concrete, elevated slab, yield line theory

Summary: *The use of steel fibres for the reinforcement of concrete structures is as competitive as higher is the support redundancy, and as many stress components develop in the structure. Slabs supported on piles or columns (here designated by elevated slabs) are this type of structures, where the statically indeterminate degree is dependent on the number of columns/piles, and five stress components are installed, three of which lead to membrane force and bending moment components, and the other two out-of-plane stresses generate the shear force components. When using relatively high content of steel fibres (1 to 1.5% in volume) of large aspect ratio (65 to 80), steel fibre reinforced concrete (SFRC) of quite significant post-crack residual tensile strength can be built, able of providing an ultimate moment much higher than its cracking moment. The benefits guaranteed by the fibre reinforcement at the cross section level are amplified at the structural level due to the stress redistribution provided by the support redundancy character of this type of structures, and by the reinforcement mechanisms assured by fibres bridging the cracks, leading to an ultimate load carrying capacity for the SFRSC slab that is much larger than the load at crack initiation. Adding the benefits of fibre reinforcement to those derived from the self-consolidating character of a self-compacting concrete (SCC), a high performance structural material can be obtained, here designated by steel fibre reinforced self-compacting concrete (SFRSCC). The behaviour of SFRSCC slab supported on columns is investigated in the present work by applying the yield line theory (YLT) to available data generated from real scale tests and performing parametric studies in order to evidence the influence of relevant parameters for the effectiveness of this innovative structural system. A SFRSCC was developed, its relevant properties were characterized, and it was used to build a 1/4 scale elevated steel fibre reinforced concrete (ESFRC) slab system prototype. The results of the first phase of the loading test program are presented.*

1 INTRODUCTION

By taking advantages of the statically indeterminate character of slabs supported on piles or columns, and the benefits from the high post-cracking residual strength of concrete reinforced with relatively high content of steel fibres (1 to 1.5% in volume) the use of steel fibre reinforced concrete

(SFRC) has recently been explored for the construction of this type of structural system. This type of slabs is generally designated by Elevated Steel Fibre Reinforced Slab (ESFRC) [1], and they include a minimum continuity rebars, also referred as anti-progressive collapse rebars, placed in the bottom of the slab in the alignment of the columns in both directions [2]. The yield line theory (YLT) has been quite used for the design of SFRC slabs supported on soil [3]. Recently, a formulation based on the YLT was developed for the design of ESFRC slabs [4]. To evaluate the plastic bending moment of the ESFRC slab cross section, the recommendations of the Model Code 2010 were adopted for the establishment of the constitutive laws of the SFRC [5]. By taking available experimental results with real scale prototypes, the predictive performance of the YL formulation is assessed in the present work. Parametric studies were executed with this formulation in order to evidence the influence of the thickness and span length of the ESFRC on its load carrying capacity. Since steel fibres are heavier than the other concrete constituents, a tendency for an increase of fibre percentage from the top to the bottom slab is generally reported, mainly when vibration conditions are applied during the cast operations [6]. To account this effect in the YLT a parameter is introduced and its influence on the load carrying capacity of ESFRC slabs is evaluated. Since this fibre distribution tendency has a negative impact in terms of slabs load carrying capacity, in the present work a steel fibre reinforced self-compacting concrete (SFRSCC) was developed, because apart the suppression of the vibration operation with the consequent economic and environmental benefits, the distribution of fibres are more homogeneous along the thickness of the slab [7, 8], resulting ESFRC slabs of larger load carrying capacity. The properties of the developed SFRSCC were characterized according to the recommendations of the Model Code 2010 and this SFRSCC was used to build a 1/4 scale prototype of an ESFRC structural system, whose geometry is represented in Figure 1. The ESFRC slab, with a length x width x thickness of 3.7×2.1×0.075 m, is supported on 12 columns of square cross section of 0.1 mm edge. The distance between columns in the X and Y directions is 1.2 m and 1.0 m, respectively.

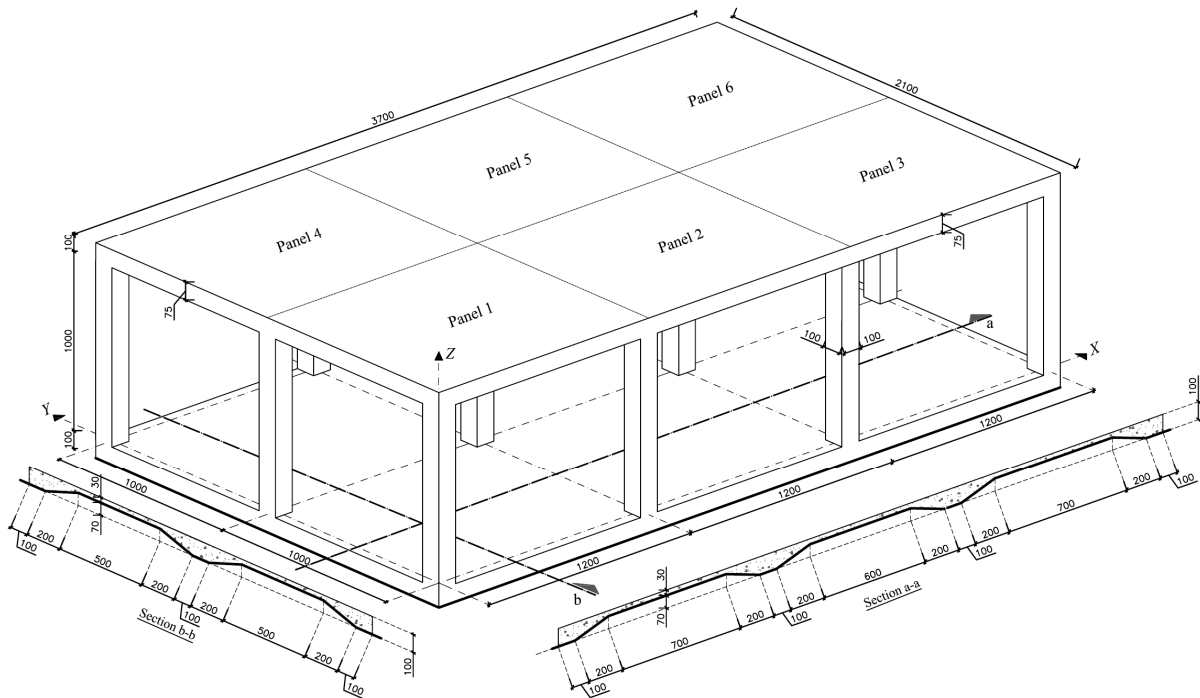


Figure 1: Geometry of the built prototype in SFRSCC (dimensions in mm).

The columns are supported on a slab on grade, whose geometry was optimized by FEM material nonlinear analysis in order to minimize the amount of SFRSCC to be applied, and to provide the formation of diffuse crack patterns in large areas of this structural element, with consequent benefits in terms of structural stability and durability. The entire prototype was built by the developed SFRSCC, and the unique conventional reinforcement is composed by four longitudinal steel bars of 6 mm diameter applied in each column. This prototype is intended to be submitted to a test program in order to investigate its behaviour for serviceability and ultimate limit states. In the present work, the preliminary results are presented, and they correspond to a loading configuration for serviceability limit states.

2 PROPERTIES OF THE SFRSCC DEVELOPED FOR THE PROTOTYPE

2.1 Composition

The SFRSCC composition indicated in Table 1, used to build the prototype, was developed by CIVITEST Company, and 90 kg/m³ of hooked steel fibres with a length, l_f , of 37 mm, a diameter, d_f , of 0.5 mm, and an aspect-ratio, l_f/d_f of 74 were used. According to the supplier this type of fibre has a tensile strength higher than 1100 MPa.

Table 1: Composition (per m³ of concrete) of the SFRSCC applied in the prototype

Cement (kg)	Water (kg)	Super plasticiser (kg)	Limestone Filler (kg)	Fly ash (kg)	Fine river sand (kg)	Coarse river sand (kg)	Crushed granite (kg)	Fibres (kg)
408	150	6.26	395	73	263	658	446	90

2.2 Properties

By performing compression tests with cylinders of SFRSCC of 28 days, with 150 mm diameter and 300 mm high, according to the standards [9], an average compressive strength, f_{cm} , of 65.96 MPa, and a Young's modulus, E_c , of 40.40 GPa were obtained. According to the Model Code 2010 [5] this concrete has an average tensile strength, f_{ctm} , of 4.30 MPa. The post-cracking behaviour of the SFRSCC was assessed by performing three-point notched beam bending tests according to the recommendations of Model Code 2010 [5], Figure 2a. This type of test provides a relationship between the applied load, F , and the crack mouth opening displacement (CMOD).

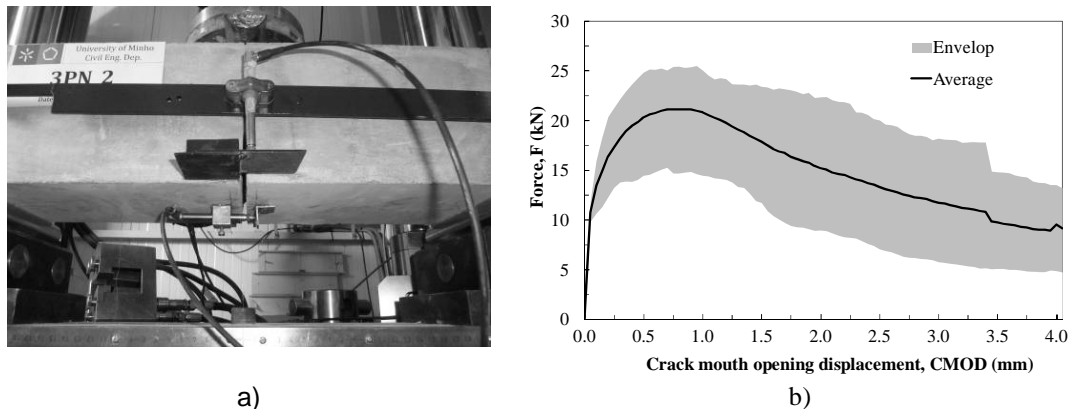


Figure 2: Three point bending test: a) set up; b) obtained force-CMOD responses

From the F - $CMOD$ it is obtained the residual flexural tensile strength parameters, f_{Rj} , for $CMOD_j$ of 0.5, 1.0, 1.5, 2.5 and 3.5 mm. According to Model Code 2010 the depth of the notch should be 25 mm. However, due to the relative high volume percentage of fibres adopted in this composition ($V_f = 1.1\%$), and in order to restrict the crack localization and propagation to the notched plane, a notch of a depth of 60 mm was introduced in the tested specimens. The envelope and the average F - $CMOD$ responses (six specimens) are represented in Figure 2b, from which the average values for the f_{Rj} , indicated in Table 2, were obtained. Since three SFRSCC batches were necessary to build the prototype, a total of 6 specimens were prepared, 2 from each batch, which can justify the relatively high standard deviation values obtained in the tests (Table 2).

Table 2: Residual strength parameters for the developed SFRSCC

Crack mouth opening displacement (mm)	Mean residual strength (MPa)
$CMOD_1 = 0.5$	$f_{R1m} = 11.99 (2.2)^*$
$CMOD_2 = 1.5$	$f_{R2m} = 10.34 (2.9)$
$CMOD_3 = 2.5$	$f_{R3m} = 7.28 (3.0)$
$CMOD_4 = 3.5$	$f_{R4m} = 5.52 (2.3)$

* () Standard deviation

3 YIELD LINE THEORY FOR THE EVALUATION OF THE LOAD CARRYING CAPACITY OF ESFRC SLABS

3.1 Formulation

In this section a brief resume of the formulation of the yield line theory (YLT) applied to ESFRC is given, but the general formulation and all the details can be found elsewhere [4]. For design purposes, bending global failure can be considered in two types of panels (Figure 3): panel interior of the slab with continuity in all the borders, and panel in the corner of the slab where two borders can be considered with simply supported conditions. Figure 3a shows the patterns of the yield lines formed in Y direction when the panels are submitted to surface load (q_{sur}), while 3b represents the pattern of the YL formed when a “point load”, distributed in a relatively small area, is applied in an interior panel. A negative YL is assumed formed by negative bending moments that correspond to the development of tensile strains in the top surface and compressive strains in bottom surface. In X direction the YL pattern is conceptually similar, but the orientation of the YL is parallel to X axis. By applying the YLT [4] it is obtained the following equations:

$$M_{py}^+ = \frac{q_{sur} \cdot L_x^2}{2(\sqrt{(1+\phi_h)} + 1)^2} \quad (\text{corner panel, surface load}) \quad (1)$$

$$M_{py}^+ = \frac{q_{sur} \cdot L_x^2}{8(1+\phi_h)} \quad (\text{Interior panel, surface load}) \quad (2)$$

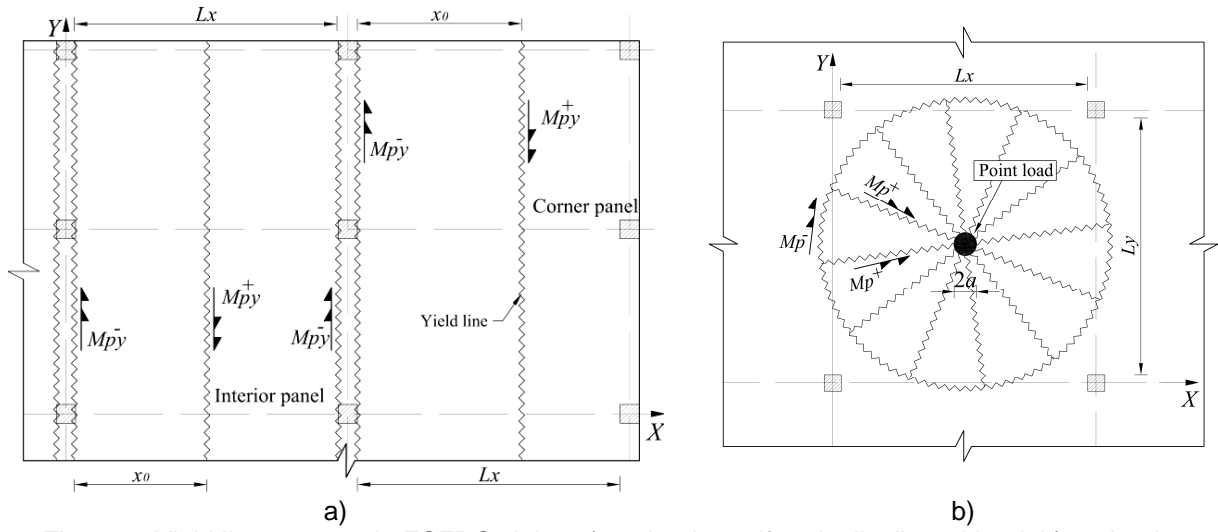


Figure 3: Yield line patterns in ESFRC slabs; a) under the uniformly distributed load, b) under the concentrated load.

$$M_p^+ = \frac{P_{poi.} \left(1 - \frac{2}{3} \frac{a}{R} \right)}{2\pi(1 + \varphi_h)} \quad (\text{Point load}) \quad (3)$$

where φ_h is the ratio of negative to positive flexural capacity of the slab cross section ($M_{py}^- = \varphi_h M_{py}^+$), which can be assumed as being equal in both X and Y directions. Available research shows a tendency for an increase of the percentage of steel fibres in the depth of the structural element, mainly when high vibration procedures are used in SFRC casting operations [6]. If SFRSCC is used, since vibration is not necessary, a more uniform fibre distribution is obtained along the depth of the element, and therefore φ_h is closer to the unit value [7, 8]. In Equation 3, a is the diameter of the equivalent area of the point load and R is the radius of the circumferential yield line that can be obtained from:

$$R = \sqrt{\frac{L_x L_y}{\pi}} \quad (4)$$

To evaluate the resisting plastic bending moment, M_p , two approaches can be used: i) defining the constitutive laws based on the recommendations of Model Code 2010 and taking the values of f_{Rj} obtained in the tests described in Section 3.2 [5], and then deriving the moment-curvature relationship using a closed form solution [10] or a cross section layer model [11]; ii) using data derived from experimental tests with round SFRC panels and applying the YLT [4]. Since in the present phase of this research program round panel tests were not yet executed, the first approach will be followed. Therefore, taking the results obtained in the three point notched beam bending tests (Table 2) and adopting the formulation proposed in the Model Code 2010 [5] the constitutive laws represented in Figure 4 are obtained, the first one (Figure 4a) if average values for f_{Rj} are adopted, and the second one (Figure 4b) if design values are assumed.

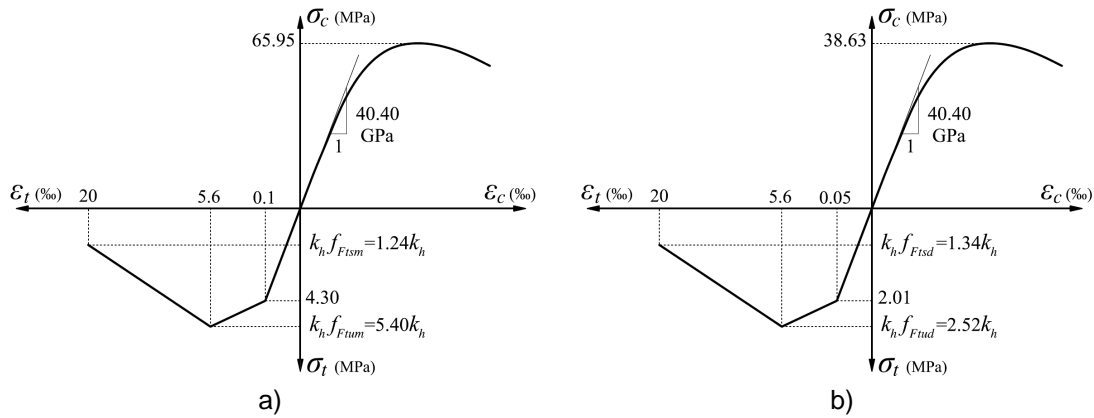


Figure 4: Constitutive laws for the developed SFRSCC adopting for f_{Rj} ; a) average, b) design values

Using these constitutive laws into DOCROS software [11], the influence of the depth of the cross section, h , on the M_p was obtained when using average values and design values for the characterization of the constitutive laws of the SFRSCC (Figure 5). In this process, to take into account the size effect on the flexural capacity of SFRSCC slabs of different h , the k_h parameter proposed by RILEM TC 162-TDF was used to re-scale the stress values corresponding to the two points that define the bilinear tensile post-cracking stress-strain diagram [12].

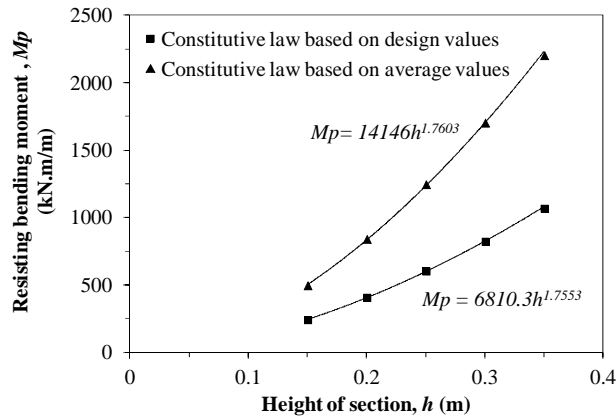


Figure 5: Variation of the positive resisting bending moment with the height of the cross section.

3.2 Predictive performance

To assess the predictive performance of the YLT applied to ESFRC, the ultimate load predicted by Equation (3) will be compared to the results obtained in two full scale tests with ESFRC structures executed in Bissen, Luxembourg [13] and Tallinn, Estonia [14]. The structure tested in Bissen consists of 3 consecutive spans of 6.0m in both X and Y directions, a flat slab of 0.2m thickness supported in columns of square cross section of 0.3m edge and free length of 2.0 m. The structure tested in Tallinn consists of 3 consecutive spans of 5.0m in both X and Y directions, a flat slab of 0.18m thickness supported in columns of square cross section of 0.3m edge and free length of 2.0 m. In both structures a C30/37 concrete strength class reinforced with 100 kg/m³ of undulated steel fibres (TABIX 13/50) of 1.3 mm diameter, 50 mm length and a tensile strength of 850 MPa were used.

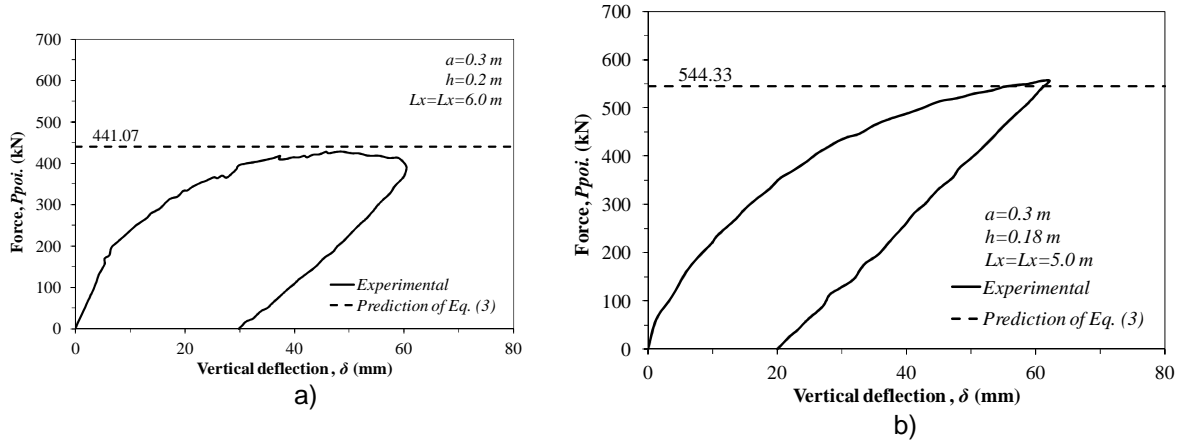


Figure 6: Force-deflection of elevated SFRC slab under point load: a) Bissen [13], b) Tallinn [14].

In both structures were also applied 3 steel bars of 16 mm in the bottom part of the slab in the longitudinal and transverse column to column directions (as anti-progressive collapse reinforcement). Both slabs were submitted to a point load applied in an interior panel. The loaded area was not indicated in the available publications, but from the photos it seems to be a square area of an edge of about 0.3m. Figure 6 represents the force versus deflection relationship obtained from these two tests. Since the only data available to characterize the SFRC applied in these two slabs is the strength class (C30/37), the resisting plastic bending moment was evaluated by adopting for the definition of the constitutive law of this SFRC the design values of the SFRSCC developed for the prototype. This is an acceptable procedure, since the design value of the compressive strength, f_{cd} , of the SFRSCC is similar to the average compressive strength, f_{cm} , of C30/37. Furthermore, in these tests the content of fibres (100kg/m^3) was a little bit higher than the fibre content applied in the SFRSCC (90kg/m^3), but in the last case the fibres have higher aspect ratio, higher tensile strength and better bond conditions to the surrounding past (hooked ends; higher strength paste). The dashed lines in Figure 6 represent the “point load” predicted by applying the YLT (Equation (3)), and a high degree of accuracy was obtained.

3.3 Parametric studies

In the following parametric studies the equation $M_{pd} = 6810h^{1.755}$ indicated in Figure 5 for evaluation of the design value of the plastic bending moment, M_{pd} , was used. The influence of the height of the slab's cross section (h) and span length (L) on the maximum surface load (applied in a corner panel), q_{sur} , and “point load” (a distributed area of $0.3 \times 0.3 \text{ m}^2$ was assumed), P_{poi} , that can be applied in ESFRC of different span lengths is represented in Figure 7a and 7b, respectively, where it was assumed $\phi_h = 1.0$. Figure 7a shows the great influence of both the h and L on the maximum surface load that can be applied to the slab, while, as expected, the span length of the slab has marginal influence of the maximum “point load” that can be applied to the slab (Figure 7b), but P_{poi} increases significantly with h . The maximum surface load is the combination of permanent loads, like the self-weight of the slab system, W_G , and other loads of permanent character (q_{PL}), and live load, q_{LL} :

$$q_{sur} = \lambda_{PL} q_{PL} + \lambda_{LL} q_{LL} = \lambda_{PL} (W_G + q_{PL}) + \lambda_{LL} q_{LL} \quad (6)$$

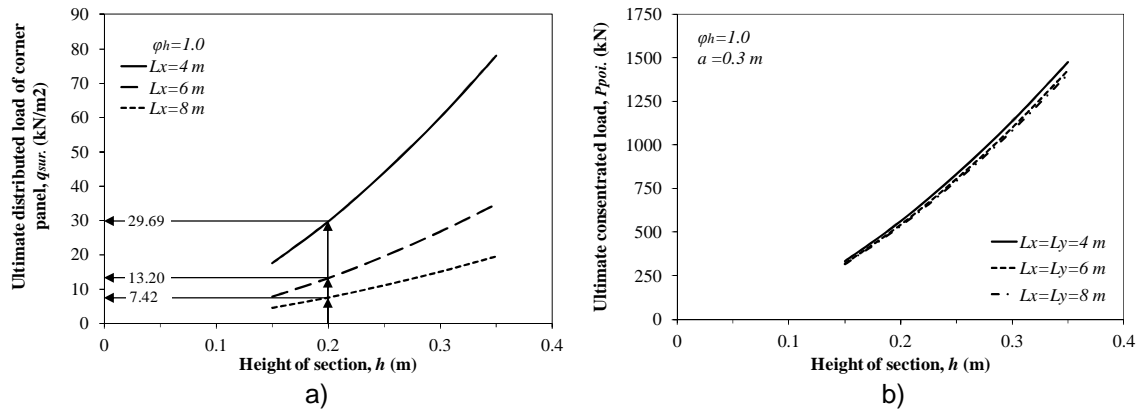


Figure 7: Influence of the height of the cross section and span length of ESFRC slab on the load carrying capacity for the loading conditions; a) uniform load on corner panel, b) concentrated load.

where λ_{PL} and λ_{LL} are load factors for permanent and live load cases, respectively, in agreement with the design codes. For the example of an ESFRC slab of $h = 0.2$ m, $q'_{PL} = 1.5$ kN/m², $\lambda_{PL} = 1.35$, $\lambda_{LL} = 1.5$, $W_G = 0.2 \times 25 \text{ kN/m}^3 = 5.0$, a q_{sur} of 7.42, 13.2 and 29.69 kN/m² is obtained for $L_x = 8, 6$ and 4 m, respectively (Figure 7a). If these values are replaced in equation (6) it is verified that it is not possible to build a slab with a span length of 8 m (a negative value is obtained for q_{LL}), while for slabs of $L_x = 6$ and 4 m a q_{LL} of 2.95 and 13.85 kN/m² can be applied, respectively.

The influence of ϕ_h for a ESFRC slab system of a span length of 6 m and different height of the cross section is represented in Figure 8a and 8b for the surface load applied in a corner panel and “point load”, respectively. Both graphs show that q_{sur} and P_{poi} decrease with the decrease of ϕ_h , and the decrease tendency is similar in both loading conditions. For the example of a ESFRC slab of $h = 0.25$ m, $L_x = 6.0$ m, $q'_{PL} = 1.5$ kN/m², $\lambda_{PL} = 1.35$, $\lambda_{LL} = 1.5$, $W_G = 0.25 \times 25 \text{ kN/m}^3 = 6.25$ kN/m², when the ϕ_h factor decreases from 1.0 to 0.6 the q_{sur} decreases from 26.83 to 21.46 kN/m². If these values are replaced in equation (6) it is obtained the following values for q_{LL} : 10.91, and 7.33 kN/m².

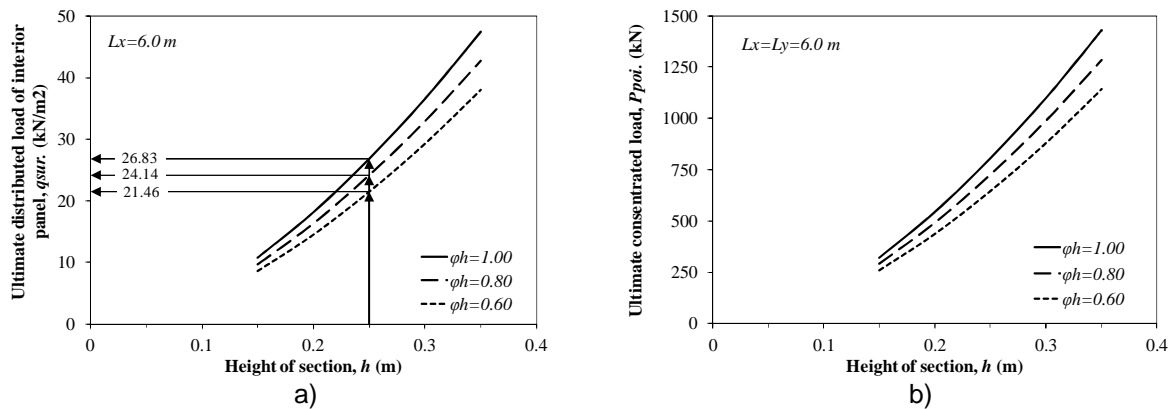


Figure 8: Influence of the height of the cross section of ESFRC slab and ϕ_h factor on the load carrying capacity for the loading conditions; a) uniform load on corner panel, b) concentrated load.

Since SFRSCC assures higher ϕ_h factors than conventional SFRC [7, 8], the higher costs of the former concrete can be compensated by a reduction on the thickness of the slab or an increase of the span length or the live load that can be applied to the slab.

4 CONSTRUCTION OF A ESFRC PROTOTYPE STRUCTURE AND PRELIMINARY TESTS

4.1 Construction

In this section is described the main steps adopted in the construction of the ESFRC prototype of $\frac{1}{4}$ scale, which geometry is described in Figure 1. The maximum deformability recorded in the tests for load conditions corresponding to serviceability limit states is also presented. The main phases of the construction process are shown in Figure 9. The SFRSCC with properties described in Chapter 2 was used. 10 days before casting the SFRSCC slab on grade, a layer of 0.15 m thickness of low strength plain concrete that was casted in order to regularize the support conditions for the slab on grade.

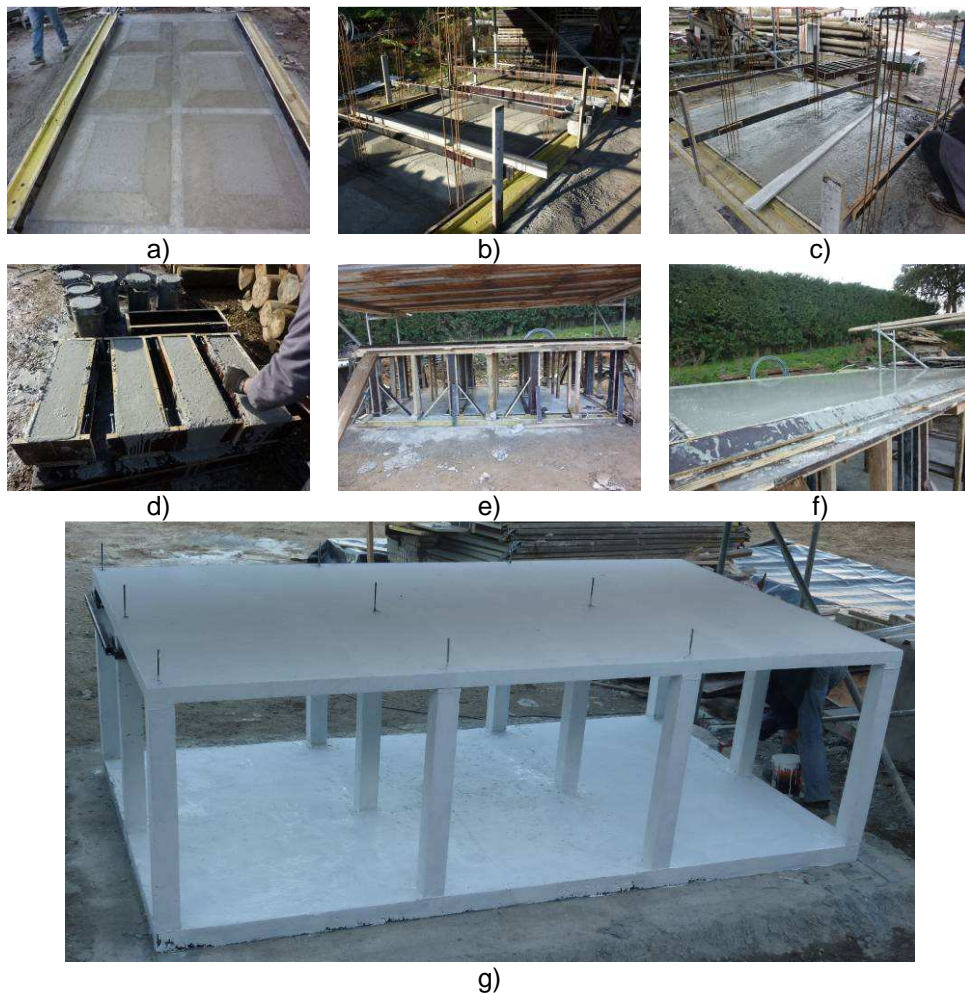


Figure 9: The construction ESFRC prototype: (a) preparation of the foundation for the slab on grade; (b) Reinforcement of the columns; (c) casting the slab on grade (1st batch); (d) casting the SFRSCC specimens; (e) casting the columns (2nd batch); (f) casting the elevated slab; (g) final appearance of the prototype after has been painted.

The geometry of the slab on grade was optimized by performing FEM material nonlinear analysis. Therefore, in the alignments of the columns exists a grid that has a constant thickness of 0.1m in the width of the columns and a linear reduction of thickness up to 0.03m that is the thickness of the interior SFRSCC panels of the slab of grade. This smooth transition of thickness promotes the formation of diffuse crack patterns in all the panels, avoiding the localization of cracks in the transition between the grid and the interior panels. In the second phase the columns, only reinforced with 4 longitudinal bars of 6 mm diameter, were cast. Due to the relative large length of the fibres (35 mm), when taking into account the cross section of the columns ($0.1 \times 0.1 \text{ m}^2$) and the concrete cover of the longitudinal reinforcement (10 mm), external vibration was necessary to apply. The third phase was composed by the casting of the SFRSCC elevated slab of 0.075 m of thickness and without any type of conventional reinforcement.

4.2 First phase of the loading test program

The first phase of the loading test program comprises the behaviour of the prototype when submitted to a loading level (uniform distributed load) corresponding to the serviceability limit states (SLS). If $q_{PL} = 1.5 \text{ kN/m}^2$ and $q_{LL} = 2.0 \text{ kN/m}^2$ is assumed for SLS, the $q_{sur.}$ is 3.5 kN/m^2 . These loading conditions were materialized by introducing water in two tanks (Figure 10a) of 1 m^3 capacity and cross section $1.1 \times 1.0 \text{ m}^2$, positioned on panels 2 and/or 3 (see Figure 1). A frame of steel elements fixed in the top part of the columns was used to install 8 LVDTs for the measurements of the vertical displacements of the slab (Figure 10b and c). The loading process of this first phase was composed by the following steps: panel 2 was firstly loaded by $q_2 = 2.09 \text{ kN/m}^2$ (0.24 m^3 water) with an average rate of 0.005 kN/s ; in the second step the load corresponding to panel 2 was incremented with an average loading rate of 0.003 kN/s up to $q_2 = 3.51 \text{ kN/m}^2$; in the third and fourth steps of loading, the tank on panel 3 was filled up to attain $q_3 = 2.30 \text{ kN/m}^2$ and $q_3 = 3.73 \text{ kN/m}^2$, respectively.

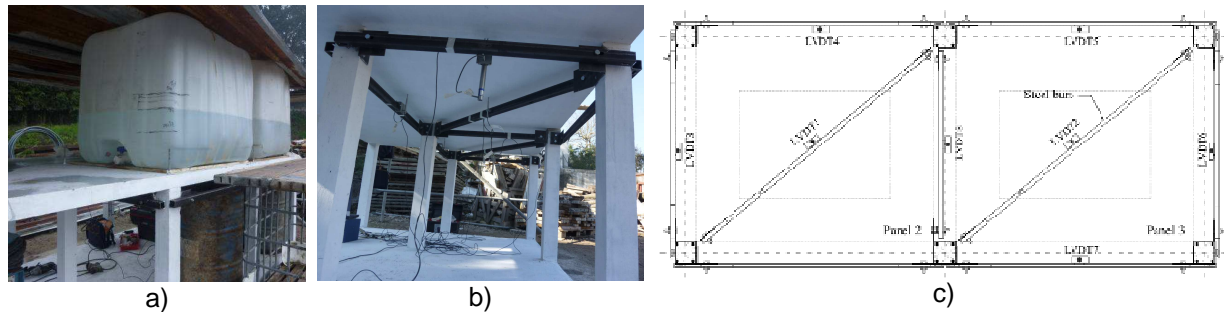


Figure 10: Test apparatus: a) Water tanks utilized for loading, b) Steel frame for the supporting of the LVDTs, c) The designation and position of the LVDTs.

Figure 11 represents the relationship between the displacements recorded in the LVDTs in the centre of the panels 2 and 3, respectively LVDT1 and LVDT2, and the applied distributed load, for the four loading steps. In these graphs the relationship predicted by a FEM analysis is also indicated (the vertical displacements are represented in Figure 12). The irregularities recorded in the displacements can be justified by the temperature variation in the steel elements and in the slab during this loading phase where the displacements are quite small. Since this temperature variation was not measured, it was not considered in the FEM simulations. As expected, for loading levels corresponding to serviceability states the structure is behaving in linear behaviour without formation of any crack. In these simulations the properties for the SFRSCC indicated in section 2.2 were used. The elevated slab was simulated by Mindlin-shell elements of 8 nodes with a Gauss-Legendre (G-L) integration

scheme of 2x2 integration points (IP), while the columns and the slab supported on grade were modelled by solid elements of 20 nodes with 2x2x2 IP.

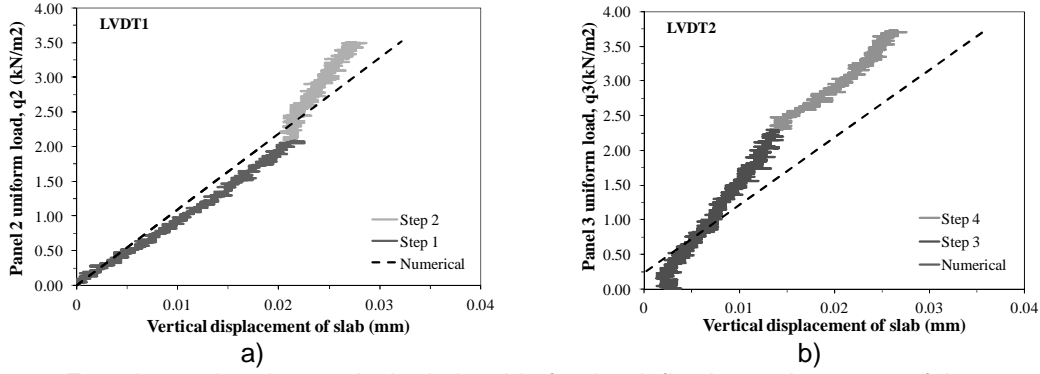


Figure 11: Experimental and numerical relationship for the deflection at the centre of the panels 2 (a) and (b) versus applied uniformly distributed load.

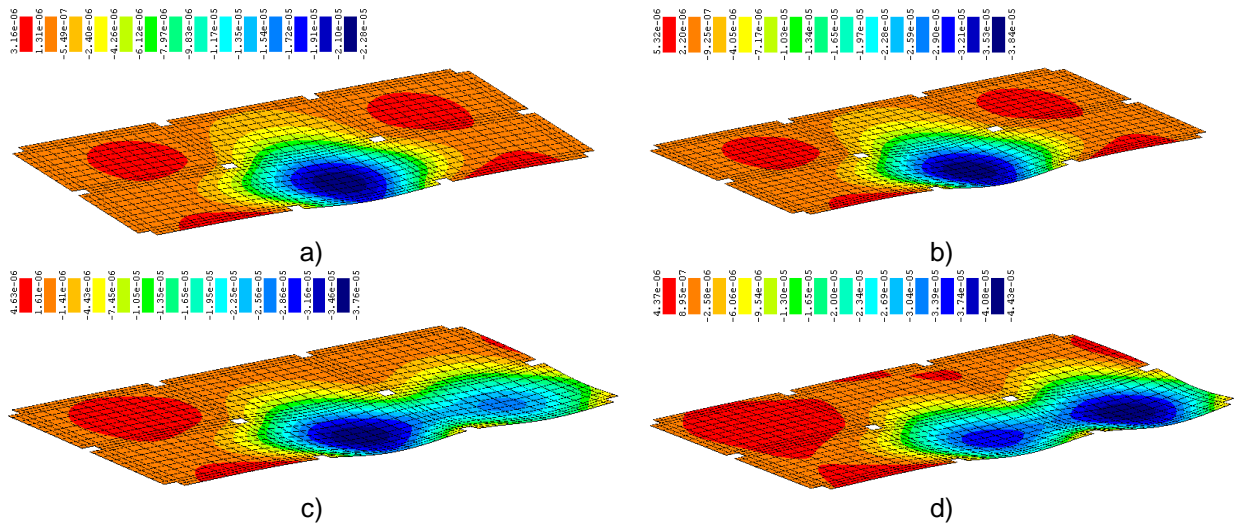


Figure 12: Representation of the vertical displacements (m) in the slab of the prototype for the four steps of the loading process: a) 1st, b) 2nd, c) 3rd, and d) 4th. (in m)

7 CONCLUSIONS

In this paper a formulation based on the yield line theory (YLT) was proposed for the design of steel fibre reinforced concrete (SFRC) slabs supported on columns, herein designated by elevated SFRC, with the acronym of ESFRC. The good predictive performance of this formulation was assessed by using available data from two full scale tests. By performing parametric studies with this formulation, the relevance of the influence of the depth of the slab's cross section and span length on the maximum surface load that can be applied to the slab was evidenced, and design examples were executed for this purpose. Since the distribution of fibres has a tendency to increase from the top to the bottom surfaces of the slab, a parameter, in this respect, was introduced in the formulation and its detrimental effect on the load carrying capacity of an ESFRC slab was evidenced. This fibre

distribution tendency is higher when SFRC is cast with vibration, and more uniform fibre distribution was reported when using steel fibre reinforced self-compacting concrete (SFRSCC). Therefore, in the present work a SFRSCC was developed with properties suitable for the construction of residential buildings based on the concept of ESFRC slabs. The relevant properties of this SFRSCC were determined from experimental programs following the recommendations of Model Code 2010. This SFRSCC was used to build a ¼ scale ESFRC prototype, and its deformational behaviour under loading conditions corresponding to serviceability limit states was assessed, which is the first phase of a test program for the evaluation of the behaviour of this structural system in service and ultimate conditions.

ACKNOWLEDGEMENTS

The study presented in this paper is a part of the research project titled SlabSys-HFRC with reference number PTDC/ECM/120394/2010. The authors also thank the collaboration of the following companies: Casais for the execution of the prototype; CiviTest for the design of the SFRSCC, the Maccaferri and RADMIXTM for supplying the fibres, and Secil and SIKA for providing the Cement and the superplasticizers, respectively.

REFERENCES

- [1] X. Destrée, "Structural application of steel fibres as only reinforcing in free suspended elevated slabs: conditions – Design examples", Sixth RILEM Symposium on fibre reinforced concrete Varenna/Italy, 2, 1073-1082, (2004).
- [2] M. Sasani and S. Sagiroglu, "Progressive collapse of reinforced concrete structures: a multihazard perspective", ACI Structural J., 105(1), 96-105, (2008).
- [3] J.A.O. Barros, A.V. Gouveia, J.M. Sena-Cruz, A.F.M. Azevedo, and J.A.B. Antunes, "Design methods for steel fibre reinforced concrete industrial floors", Third Int. Conf. Construction Materials: Performance, Innovations and Structural Implications, CD, Vancouver, Canada (2005).
- [4] H. Salehian, J.A.O., Barros, "Design of elevated steel fibre reinforced self-compacting concrete slabs", Technical report 11-DEC/E-30, Department of Civil Engineering, School Engineering, University of Minho (2011).
- [5] Model Code 2010, Final draft, fib, (2011).
- [6] J.A.O. Barros and J.A.B. Antunes, "Experimental characterization of the flexural behaviour of steel fibre reinforced concrete according to RILEM TC 162-TDF recommendations", RILEM TC 162 TDF Workshop, 77-89, (2003).
- [7] V.M.C.F. Cunha, "Steel fibre reinforced self-compacting concrete: from micro-mechanics to composite behaviour", PhD Thesis, University of Minho, Guimaraes, Portugal, (2010).
- [8] F.L. Oliveira, "Design-oriented constitutive model for steel fibre reinforced concrete", PhD Thesis, Universitat Politècnica de Catalunya, Barcelona, Spain (2010).
- [9] EN 206-1, "Concrete - Part 1: Specification, performance, production and conformity." European standard, CEN, 69, (2000).
- [10] M. Taheri, J.A.O. Barros, H. Salehian, "A design model for strain-softening and strain-hardening fibre reinforced elements reinforced longitudinally with steel and FRP bars", Composites - Part B J., 42, 1630-1640, (2011).
- [11] C.A.A., Basto and J.A.O., Barros, "Numeric simulation of sections submitted to bending", Technical report 08-DEC/E-46, Department of Civil Engineering, School Engineering, University of Minho, Guimaraes, Portugal, (2008).
- [12] L. Vandewalle et al., "Test and design methods for steel fibre reinforced concrete – σ - ϵ design method - Final Recommendation", Materials and Structures, 36(262), 560-567, (2003).
- [13] B. Espion, "Test report n°33396", University of Brussels, Belgium, (2004).
- [14] J. Mandl, "Flat slabs made of steel fibre reinforced concrete (SFRC)", CPI worldwide, 1, (2008).